Probing the Diphosphoglycerate Binding Pocket of HbA and HbPresbyterian (β108Asn → Lys)[†]

David S. Gottfried,*[,‡] Belur N. Manjula,[‡] Ashok Malavalli,[§] A. Seetharama Acharya,[§] and Joel M. Friedman[‡]

Department of Physiology and Biophysics and Department of Medicine, Division of Hematology, Albert Einstein College of Medicine, 1300 Morris Park Avenue, Bronx, New York 10461

Received November 18, 1998; Revised Manuscript Received June 24, 1999

ABSTRACT: HbPresbyterian (β108Asn → Lys, HbP) contains an additional positive charge (per $\alpha\beta$ dimer) in the middle of the central cavity and exhibits a lower oxygen affinity than wild-type HbA in the presence of chloride. However, very little is known about the molecular origins of its altered functional properties. In this study, we have focused on the $\beta\beta$ cleft of the Hb tetramer. Recently, we developed an approach for quantifying the ligand binding affinity to the β-end of the Hb central cavity using fluorescent analogues of the natural allosteric effector 2,3-diphosphoglycerate (DPG) [Gottfried, D. S., et al. (1997) *J. Biol. Chem. 272*, 1571−1578]. Time-correlated single-photon counting fluorescence lifetime studies were used to assess the binding of pyrenetetrasulfonate to both HbA and HbP in the deoxy and CO ligation states under acidic and neutral pH conditions. Both the native and mutant proteins bind the probe at a weak binding site and a strong binding site; in all cases, the binding to HbP was stronger than to HbA. The most striking finding was that for HbA the binding affinity varies as follows: deoxy (pH 6.35) > deoxy (pH 7.20) > CO (pH 6.35); however, the binding to HbP is independent of ligation or pH. The mutant oxy protein also hydrolyzes *p*-nitrophenyl acetate, through a reversible acyl−imidazole pathway linked to the His residues of the $\beta\beta$ cleft, at a considerably higher rate than does HbA. This implies a perturbation of the microenvironment of these residues at the DPG binding pocket. Structural consequences due to the presence of the new positive charge in the middle of the central cavity have been transmitted to the $\beta\beta$ cleft of the protein, even in its liganded conformation. This is consistent with a newly described quaternary state (B) for liganded HbPresbyterian and an associated change in the allosteric control mechanism.

Many anions and small molecules (effectors) modify the oxygen binding properties of hemoglobin (Hb)[1] through interactions with the water-filled domains of the protein. Such effector-induced alterations of Hb's oxygen affinity are thought to arise from preferential binding of the effector to a particular quaternary state which shifts the equilibrium between high- and low-affinity structures. In most cases, the population of the low-affinity T (deoxy) quaternary state is favored by the presence of the effector molecules which decreases the oxygen affinity of the Hb solution (*1*). The binding pocket for the allosteric effector 2,3-diphosphoglycerate (DPG), whose binding lowers the oxygen affinity of HbA within the red blood cell, is located among a cluster of eight positive charges at the β end of the central cavity that is more accessible in the T state. Previous studies have also indicated that some effectors can bind to the ligand-bound states of Hb and thus potentially affect the structure and properties of the canonical R state (*2*−*5*).

Hemoglobin Presbyterian (HbP) is a naturally occurring single-site (per $\alpha\beta$ dimer) mutant (β108 Asn → Lys) (*6*). In the presence of chloride ions, this hemoglobin variant has a substantially reduced oxygen affinity (as measured by values of P_{50}) with normal cooperativity, compared to wild-type HbA, whereas in the absence of chloride HbP and HbA have nearly identical oxygen affinities. The mechanism whereby binding of chloride is communicated to the oxygen binding sites at the heme groups has not been determined. However, the influence of the β108 Asn → Lys substitution is muted when the protein is cross-linked at its DPG binding pocket using bis-sulfosuccinimide suberate (*7*). A comparative mapping of the various functional and structural domains of the mutant protein and an integration of such structural information are critical to establishing the molecular basis of the chloride-induced low oxygen affinity of this protein. HbP is currently involved in continuing investigations of hemoglobin-based, acellular oxygen carriers (blood substitutes) (*8*). In addition, the added positive charge in a key region of the central cavity has made HbP a focus of studies undertaken to better understand both allosteric transitions and the communication pathways between the effector binding site and the oxygen binding sites at the heme moieties (*7*).

A recent X-ray crystallographic study has revealed a new T-like structure, designated the B state, for a liganded

[†] This work was supported by grants from the National Institutes of Health (PO1HL51084 and RO1HL58247) and the W. M. Keck Foundation.

* To whom correspondence should be addressed. Current address: Georgia Tech Research Institute, 925 Dalney St., Atlanta, GA 30332. E-mail: David.Gottfried@eoeml.gtri.gatech.edu.

[‡] Department of Physiology and Biophysics.

[§] Department of Medicine, Division of Hematology.

[1] Abbreviations: DPG, 2,3-diphosphoglycerate; fwhm, full width at half-maximum; Hb, hemoglobin; HbA, human hemoglobin A; HbP, human hemoglobin Presbyterian (β108Asn → Lys); HPTS, 8-hydroxy-1,3,6-pyrenetrisulfonate; IEF, isoelectric focusing; IHP, inositol hexaphosphate; IRF, instrument response function; *p*-NPA, *p*-nitrophenyl acetate; PBS, phosphate-buffered saline; PyTS, 1,3,6,8-pyrenetetrasulfonate.

10.1021/bi9827464 CCC: $18.00
Published on Web 08/12/1999

derivative of a cross-linked HbP variant (*9*). This variant, designed as a blood substitute, differs from normal HbP by the presence of a glycine bridge between the C-terminus of one α chain and the N-terminus of the other α chain, as well as the substitution of methionine instead of valine at the N-termini of both globin chains. It is not certain to what extent the cross bridge contributes to the stabilization of the new structure. This new structure determined for the cyanomet HbP variant is distinctive from both the classic R structure (*10*) and several recently described liganded R-like structures [R2 (*11*) and Y (*12*)]. As in the different liganded R structures, the heme ligand binding sites do not appear strained. Nonetheless, the overall conformation of the central cavity in the B structure is T-like. Most significant is the fact that the DPG binding site, normally closed to effector binding in the liganded R quaternary state (*10*) and open in the deoxy T state (*13*), is open and accessible in the new liganded B state. If this quaternary structure is characteristic of liganded HbP, and not due to the glycine bridge, then it would be expected that liganded HbP would also have an open DPG pocket and conceivably a higher affinity for DPG site substrates than liganded HbA.

In this study, we tested the above hypothesis on solution-phase HbP derived from transgenic swine. A novel method for quantification of free and bound ligand, based on fluorescence lifetimes of a DPG analogue, was used to compare the binding affinity of the $\beta\beta$ cleft in the deoxy and CO ligation states of HbA and HbP. In addition, the Hb-catalyzed hydrolysis of *p*-nitrophenyl acetate, associated with the β2His and β82Lys residues located in the $\beta\beta$ cleft (*14*, *15*), provides additional information regarding the conformational and electrostatic changes due to the mutation in the central cavity of HbPresbyterian.

The effector binding at the $\beta\beta$ cleft of the Hb tetramer is difficult to probe directly since both the common effectors that bind there (naturally occurring DPG and the commonly used inositol hexaphosphate), as well as the coordinating protein residues, are spectroscopically silent. Gibson and colleagues (*16*, *17*) demonstrated that a pyrene derivative, 8-hydroxy-1,3,6-pyrene trisulfonate (HPTS, also known as pyranine), binds to the DPG site and mimics the functional characteristics of the allosteric effectors DPG and IHP. The binding of the probe was confirmed and quantified by the drastic reduction in its fluorescence intensity due to quenching by the nearby heme groups. In a recent study (*4*), we showed that the measurement of the probe's time-resolved fluorescence is a useful extension of this technique. The fluorescence intensity can be fit to a decay model consisting of distinct populations of emitting probe molecules each with a resolvable lifetime. In particular, since at each concentration of added ligand the absolute fractions of bound and free ligand are determined, there is no need to rely on saturation of the binding site to provide the maximal change in the fluorescence intensity. As will be shown, the spectra of the individual species (free and bound) can be measured as well. Finally, nonspecific binding of the probe can be monitored and excluded from the titration analysis. This study is distinct from that reported earlier in that a different pyrene derivative, 1,3,6,8-pyrenetetrasulfonate (PyTS), was used to eliminate the effects of the photoexcited proton-transfer reaction of HPTS.

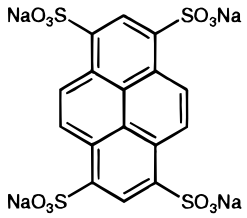

FIGURE 1: Chemical structure of 1,3,6,8-pyrenetetrasulfonate (PyTS), a fluorescent DPG analogue.

MATERIALS AND METHODS

Materials. The fluorophore PyTS (Figure 1) was purchased from Molecular Probes and used without further purification. The concentration of the probe in bis-tris buffer solution was determined by absorption spectroscopy using the extinction coefficient of 48.7 mM^{-1} cm^{-1} at 375 nm.

Hemoglobin A was prepared from erythrocytes obtained from the whole blood of an AA individual. The cells were washed with phosphate-buffered saline (PBS) at pH 7.4 and lysed using an equal volume of distilled water. The lysate was freed from the cell debris by centrifugation and dialyzed against 0.05 M tris-acetate buffer at pH 8.3. HbA was purified from the lysate on DE-52 which was developed using a pH gradient (pH 8.3 to 7.3). The main HbA peak, identified by reverse-phase HPLC (RPHPLC) and isoelectric focusing (IEF), was isolated and rechromatographed on CM-52. HbA was eluted with a linear pH and ionic strength gradient using equal volumes of 10 mM phosphate buffer (pH 6.5) and 15 mM phosphate buffer (pH 8.3). HbPresbyterian was purified from the erythrocytes of transgenic swine expressing the mutant hemoglobin (DNX Biotherapeutics, Inc.). Hemolysate was prepared as described for HbA and purified on DE-52 with a pH gradient (pH 8.1 to 7.3). HbP elutes from the column earlier in the gradient than HbA with a >95% purity as analyzed using RP-HPLC and IEF.

Concentrated solutions of the proteins were dialyzed against 50 mM bis-tris buffer for both pH 7.2 and 6.35 samples. COHb was prepared by gently passing chemically pure carbon monoxide gas over the surface of the Hb solution. DeoxyHb was obtained by passing pure nitrogen gas into an anaerobic vessel containing the Hb solution which was then anaerobically transferred to a fluorescence cuvette containing 1−2 equiv of sodium dithionite. For deoxy samples, aliquots of PyTS were also added under a nitrogen atmosphere. Complete conversion to the CO or deoxy forms was verified by the absorption spectrum, and the concentrations of both HbA and HbP were determined using the extinction coefficients (per heme) of 13.4 mM^{-1} cm^{-1} at 540 nm (CO) and 12.5 mM^{-1} cm^{-1} at 555 nm (deoxy) (*18*).

Time-Resolved Fluorescence Measurements. The fluorescence lifetime of the PyTS probe was measured using time-correlated single-photon counting as described previously (*4*, *19*). For front-face fluorometry, the optically dense sample was placed in a triangular quartz cuvette which was rotated such that the direction of excitation was 34° with respect to the surface normal (*20*). Emission at 400 nm (excitation at 355 nm) was collected through a subtractive double monochromator (16 nm spectral bandwidth) and digitized using an analog−digital converter/multichannel analyzer. For some experiments, 285 nm excitation was used, and the PyTS emission was found to be independent of the excitation

wavelength. The instrument response function was typically 32 ps [full width at half-maximum (fwhm)]. Time-gated fluorescence spectra were obtained by step-scanning the monochromator while counting only those emission events at each wavelength that fall into a predefined temporal region of interest in the fluorescence decay. In this manner, spectra with a time resolution of ~100 ps could be measured.

Titration Data Analysis. Decays were fit to a discrete sum of exponentials using a nonlinear, least-squares fitting routine (Marquardt algorithm):

$$I(t) = \alpha_b \exp(-t/\tau_b) + \alpha_n \exp(-t/\tau_n) + \alpha_f \exp(-t/\tau_f) \quad (1)$$

where the α_i values are the pre-exponential factors (amplitudes) and the τ_i values are the fluorescence lifetimes. Determination of the quality of fit was judged from the value of the reduced χ^2, the runs test, the residuals, and the autocorrelation of the residuals (*21*). Estimation of the error in the fitting parameters was carried out using the support plane method (χ^2 surface) (*22*).

The lifetime components (b being bound, n nonspecific, and f free) were assigned to individual probe populations on the basis of the expected quenching due to binding of the probe in the vicinity of the heme moieties and the observed dependence on probe concentration (*4*). The shortest lifetime component ($\tau_b = 25-35$ ps) is assigned to the PyTS probe bound to the DPG site. Previous results from our group and others (*4*, *16*, *17*, *23*) using the comparable probe HPTS have demonstrated, through competitive displacement by 2,3-diphosphoglycerate and inositol hexaphosphate (IHP), that the pyrene-based probes do bind to the DPG site at the β end of the central cavity. The longest lifetime component ($\tau_f \sim 6$ ns) arises from the PyTS free in solution.[2] Last, an intermediate lifetime component ($\tau_n = 200-500$ ps) has previously been assigned to contributions from nonspecifically bound probe (*4*).

As will be shown, the emission spectrum is invariant with binding of the probe, allowing the amplitude factors (α_i) to be used directly to calculate the fractional concentrations of the probe in the different populations. These amplitudes are equated to their fractional population in the sample and the titration data fit to the independent, nonequivalent, two-binding site model (*24*):

$$B = \frac{B_{max}^{(1)} F}{K_d^{(1)} + F} + \frac{B_{max}^{(2)} F}{K_d^{(2)} + F} \quad (2)$$

where B and F are the bound and free probe concentrations, respectively, $K_d^{(i)}$ values are the equilibrium dissociation constants, and $B_{max}^{(i)}$ values are the binding site concentrations for each distinct value of K_d.

Esterase Activity Measurements. Kinetic studies of the hydrolysis of *p*-nitrophenyl acetate (*p*-NPA), obtained from Sigma and used without further purification, were performed at room temperature (23 °C) in a Shimadzu double-beam spectrophotometer measuring the increase in absorption at 400 nm due to the production of *p*-nitrophenol. A stock solution of *p*-NPA (generally 50 mM) was freshly prepared in acetone on the day of use and kept cold in an ice bath. The esterase activities of oxygen-ligated HbA and HbP were measured in phosphate-buffered saline at pH 7.4 unless otherwise noted. The extent of hydrolysis of *p*-NPA in the buffer alone was measured continuously for a period of about 6 min to serve as a control for the Hb-mediated hydrolytic reaction. The progress of the hydrolysis of *p*-NPA in the presence of Hb was corrected by subtracting the extent of buffer hydrolysis and expressed as the change in absorption at 400 nm. The esterase activity was determined at least twice for each protein concentration (3−15 μM). To establish the influence of the phosphate and chloride concentrations on the esterase activity, phosphate buffers with a specific molarity and 10 mM phosphate buffer containing the desired amount of sodium chloride were prepared and used in place of the usual PBS buffer.

To determine whether the irreversible or reversible hydrolytic pathway is influenced by the presence of β108Lys in HbP, protein samples were incubated with *p*-NPA at concentrations approximately 10 times higher than that used for the kinetic studies. After reaction for 30 min, the proteins were subjected to gel filtration on a Sephadex G-25 column equilibrated with PBS. This separates Hb from the reagents and the hydrolysis products. The Hb peak was pooled, concentrated, and then subjected to isoelectric focusing. The isoelectric focusing of the Hb samples was carried out using precast Resolve gels from Isolab. The samples were applied to the agarose IEF gels with a blend of pH 6−8 Resolve ampholytes and electrofocused for 45 min to separate the components in the sample.

RESULTS

Lifetime-Detected PyTS Titration. A typical set of titration data (deoxyHbA, pH 6.35) for a protein concentration of 160 μM in tetramer and probe at concentrations in the range of 22−300 μM is shown in Figure 2. The data clearly illustrate the multiple lifetime components corresponding to the molecular species described above and the changes in their relative populations. As the concentration of PyTS increases and the binding sites become saturated, the fraction of free probe (indicated by the amplitude of the long-lived tail of the fluorescence decay) increases. The short lifetime of the bound species is the result of quenching by the heme groups.

The assignment of the short lifetime component in the PyTS fluorescence intensity decay is based on several pieces of evidence. First, substantial previous work by Gibson and co-workers (*16*, *17*), using the closely related probe HPTS, has identified the binding site as the DPG pocket in the $\beta\beta$ cleft of the Hb central cavity. We have previously confirmed this conclusion using time-resolved fluorescence measurements (*4*). Competitive binding experiments with IHP, which is known to bind preferentially to the DPG site, show displacement of PyTS from its binding site as judged by the decrease in the amplitude of the quenched emission component (see below). Last, the oxygen affinity of Hb is reduced in the presence of PyTS, consistent with its binding to an allosteric effector site (C. Bonaventura, personal communication).

Invariance of the Probe Spectrum. To ensure that the pre-exponential factors can be used to represent the true

[2] The actual value of the PyTS fluorescence lifetime in the absence of protein was found to be slightly higher than that of the free population in the binding experiments. The reduction in the value of the free probe lifetime in Hb solution is probably due to excited state collisional quenching with the high concentration of protein molecules.

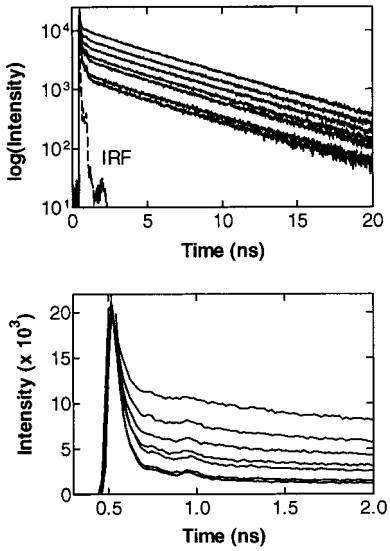

FIGURE 2: Example of time-resolved fluorescence from PyTS titrated into a solution of deoxyHbA [0.17 mM tetramer in 50 mM bis-tris (pH 6.35)]. The top panel shows the fluorescence decay curves for seven PyTS concentrations [22 (bottom) to 300 μM (top)] on a logarithmic intensity scale. The bottom panel expands the time axis and displays the data on a linear intensity scale. Emission was collected at 400 nm (16 nm spectral bandwidth) with excitation at 355 nm. IRF is the instrument response function.

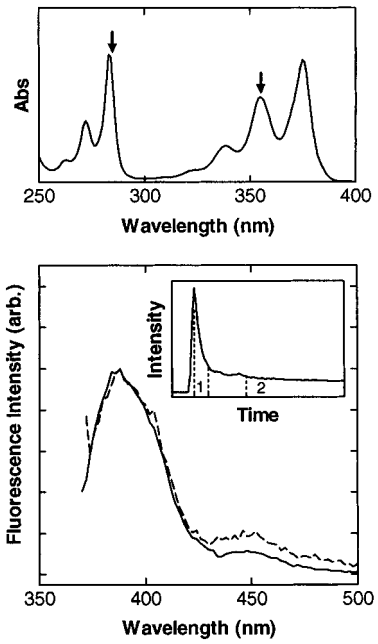

FIGURE 3: Time-gated spectra of PyTS (5 μM) in a solution of deoxyHbA [0.16 mM tetramer in 50 mM bis-tris (pH 7.2)]. The top panel shows the absorption spectrum of PyTS (in water) with 285 and 355 nm (excitation wavelengths used in this study) denoted with arrows. The emission spectra (excitation at 355 nm) were collected for time ranges of 0−100 ps (− − −) and 500 ps to 20 ns (—). The inset shows these time ranges displayed schematically on a decay curve labeled as regions 1 and 2, respectively.

populations in a quantitative manner, the emission spectra of the solution-phase PyTS must not be altered by its binding to the protein. If that were the case, then the measured fractional populations would depend on the observation wavelength, which is an undesirable complication in the analysis. Figure 3 shows time-gated emission spectra of the bound (time < 100 ps) and free (time > 500 ps) PyTS. These spectra were collected by scanning the emission monochromator while counting only those photons that arrive at the detector within a specified time window compared to the reference pulse from the excitation laser (set to time zero). While not a rigorous measure of the spectra of the free and bound species, because most of the emission at times of <100 ps originates from the bound fluorophore, while that observed at times of >500 ps originates from the free fluorophore, these spectra are reasonable approximations. The observation that the spectra are nearly identical, particularly in the vicinity of the detection wavelength at 400 nm, implies that the fractional populations of the three species can be extracted directly from the fitting amplitudes without correcting for spectral changes.

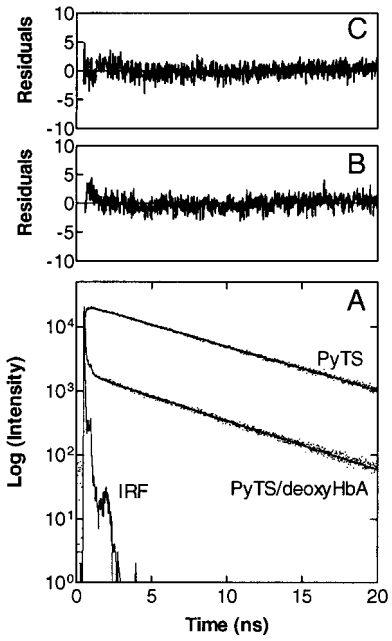

FIGURE 4: (A) Decay of free PyTS (5 μM, pH 6.35) and an example fit of one set of decay data from the titration shown in Figure 2 [44 μM PyTS and 0.17 mM deoxyHbA in 50 mM bis-tris (pH 6.35)]. The data are shown as dots, and the fits are shown as solid lines through the data. The instrument response function is labeled IRF. (B and C) Residuals for the fits to the data for PyTS in the absence and presence of deoxyHbA, respectively. For free PyTS (single-exponential), $\tau = 6.1$ ns ($\chi^2 = 1.28$). For PyTS/deoxyHbA (fit to eq 1), $\tau_b = 34$ ps, $\alpha_b = 90.5\%$, $\tau_n = 261$ ps, $\alpha_n = 5.2\%$, $\tau_f = 5.7$ ns, $\alpha_f = 4.3\%$ ($\chi^2 = 1.16$).

Fit of Decay Data. At each concentration of added probe, corresponding to a separate decay curve as shown in Figure 2, the decay is fit to the sum of exponentials whose component amplitudes are assigned to the bound, nonspecific, and free probe populations (eq 1). An example fit is shown in Figure 4 where it is compared to the single-exponential decay of PyTS in the absence of any Hb. Errors in the fractional populations are estimated by performing a rigorous error analysis. In this method, nonlinear fitting of the data is repeated for different values of a single fixed parameter and plotted against the resulting χ^2 values. The *F* test is used to calculate one and two standard deviation limits for χ^2 which then provide a confidence interval for the parameter of interest. An example of this analysis is shown in Figure 5 for the data whose fit is displayed in Figure 4.

The presence of a low concentration of heme-free Hb subunits due to the dynamic equilibrium between globin-bound and free heme has been shown to have an impact on

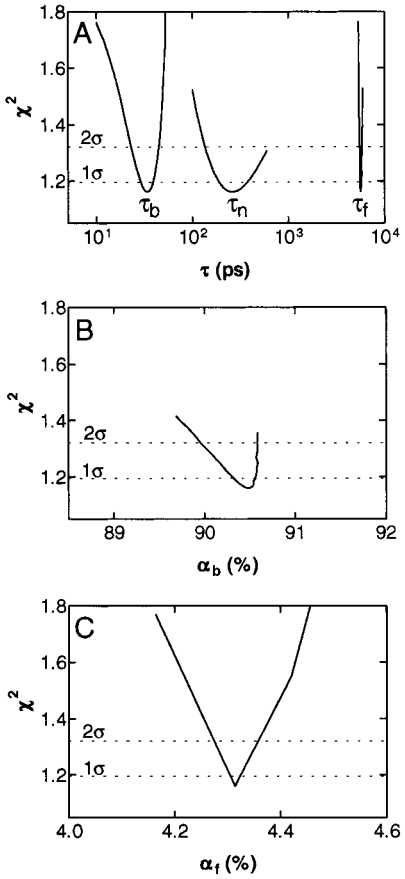

FIGURE 5: Error analysis of the fit shown in Figure 4. (A) Semilog plot showing the confidence intervals for the decay time parameters illustrating the temporal separation of the components providing for precise estimates of their amplitudes. (B and C) Confidence intervals for the bound fraction (α_b) and the free fraction (α_f) of PyTS exhibit absolute errors of much less than 1% in the recovered parameters. The two dashed lines correspond to one-standard deviation (67%) and two-standard deviation (95%) confidence intervals, respectively.

the distribution of fluorescence lifetimes from the tryptophan residues in HbA (*25*, *26*). Thus, the possibility arises that the intermediate (200−500 ps) lifetime component may result from reduced quenching of PyTS bound to the DPG site in a Hb molecule which possesses less than four heme moieties or PyTS bound directly to an empty heme pocket in a globin subunit.[3] This was tested by monitoring the PyTS lifetime component amplitudes (in the presence of HbA) upon addition of excess heme (as hemin dicyanide). No significant change is observed in the intermediate (nonspecific) component; however, with a large excess of heme, a small amount of displacement of the probe from the DPG site (short lifetime) and release into the solvent is seen (data not shown). Thus, although the exact nature of the nonspecific PyTS binding has not been determined, heme loss appears not to play a dominant role.

Binding Isotherms Reveal Two Binding Sites. In a previous report of quantitative measurements of ligand binding in the DPG pocket of COHbA at low pH, we were able to fit the titration data with a single-binding site model (*4*). That set of experiments, which used the probe HPTS, was made more difficult by the photoexcited proton-transfer reaction of this

[3] HPTS has been shown to bind reversibly to the heme pocket in apoMb (*35*).

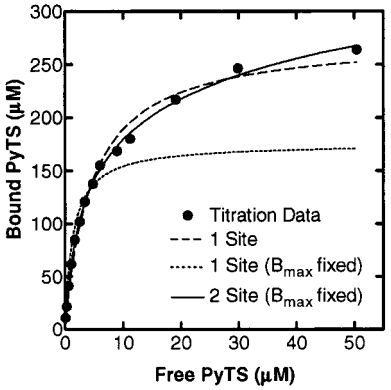

FIGURE 6: Example fit of the saturation binding data illustrating the inadequacy of a single-binding site model. Data are for PyTS binding to deoxyHbP (pH 6.35). Freedom of both the K_d and B_{max} parameters produces the dashed line fit which goes through the data but results in a value of B_{max} (275 μM) which is not in agreement with the known protein concentration (175 μM). If the B_{max} parameter is fixed to the Hb concentration in the fitting function of a single-site model, then the dotted line results, which is obviously a poor fit to the data. The best model, with only two variable parameters, is one with two independent binding sites per hemoglobin tetramer (solid line through the data points).

probe (*27*). In this study, we have examined the binding of a related pyrene, PyTS, which lacks the photoactive acidic hydroxy group. Although the data for binding of PyTS to the pH 6.35 COHbA sample could still be fit to a single-binding site model, the titration data for all the other Hb samples examined in this report required a fitting model with two independent, nonequivalent binding sites (eq 2). An example of the fitting, for deoxyHbP (pH 6.35), is shown in Figure 6. The B_{max} parameter is defined as the concentration of bound ligand when the binding site is saturated. For a single site, this is equal to the protein concentration. As can be seen, a single-binding site model with B_{max} fixed at the protein concentration is grossly inadequate for fitting the data points. However, if two separate binding sites with noncooperative binding are allowed and the individual binding site concentrations fixed at the protein concentration, then the quality of the fit is quite good. It should be noted that in this model only the values of the two dissociation constants (K_d) are variables.

Binding of PyTS to HbA and HbP. A plot of the saturation binding curves for PyTS binding to HbA and HbP under the different ligation and pH conditions is shown in Figure 7. The initial slopes of the binding curves, which are determined by the high-affinity dissociation constant, provide a qualitative means of comparing the data. The data indicate a higher affinity of the probe for HbP than for HbA under all conditions. In addition, binding of the probe to the tight binding site in HbP is nearly independent of ligation state or pH. Table 1 lists the dissociation constants for both the strong and weak binding sites from the fitting of the data shown in Figure 7 to the two-binding site model. The values of the binding affinity for HbA are consistent with those previously observed for the similar probe HPTS (*4*, *16*, *17*). As anticipated, deoxyHbA has a greater affinity for effectors at the DPG site than does liganded HbA, although at acidic pH even COHbA has measurable binding affinity. The binding affinity for the CO derivatives drops dramatically as the pH is increased. In addition, the observed increase in binding affinity for deoxyHbA as the pH is decreased from

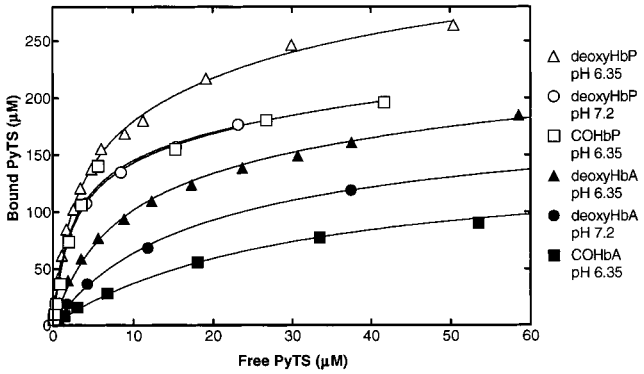

FIGURE 7: Titration data and fits for the binding of PyTS to HbA (black symbols) and HbP (white symbols). All data were fit to the two-site model, with the exception of the data for COHbA (pH 6.35) which were found to fit to a single-site model; however, the possibility of a second binding site with very weak binding affinity cannot be excluded. The values of the dissociation constants obtained from these data and fits are given in Table 1.

Table 1: Dissociation Constants (μM) for Binding of PyTS to HbA and HbP[a]

	deoxy at pH 7.2	deoxy at pH 6.35	CO at pH 6.35
HbA	15.49 ± 0.58 680.5 ± 69.5	7.40 ± 0.30 201.0 ± 14.5	29.31 ± 1.61
HbP	2.29 ± 0.087 93.23 ± 7.25	2.27 ± 0.087 38.33 ± 1.87	2.21 ± 0.238 104.10 ± 18.97

[a] All samples were in 50 mM bis-tris buffer at the indicated pH. Hb concentrations were 150−200 μM in tetramer as determined spectrophotometrically. Dissociation constants are presented as the nonlinear regression best-fit parameter ± the standard error.

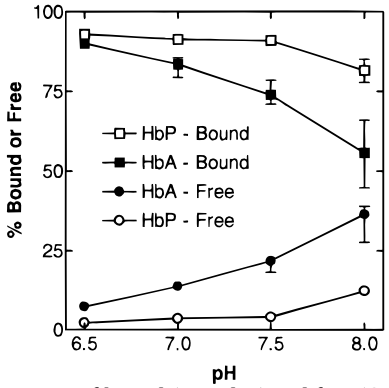

FIGURE 8: Fractions of bound (■ and □) and free (● and ○) PyTS (total concentration of 20 μM) in the presence of deoxyHbA and deoxyHbP (100 μM tetramer) as a function of pH (50 mM bis-tris; 50 mM bis-tris-tris for pH 8.0). Error bars represent the two-standard deviation (95%) confidence interval.

neutral to slightly acidic is as expected due to protonation of titratable residues in the DPG pocket.

The pH dependence of PyTS binding to the nonliganded (deoxy) proteins was further examined over the pH range of 6.5−8.0. Figure 8 shows the fractions of bound and free probe in identical solutions of 20 μM PyTS and 100 μM Hb tetramer. Between pH 6.5 and 7.5, there is no change in the extent of binding for HbP, while HbA exhibits a decreased affinity for the probe due to the titratable His residues in the $\beta\beta$ cleft. The invariance of the binding affinity in HbP with pH suggests an electrostatic and/or steric interaction between the added positive charge (β108Lys) and a titratable residue at the binding site whose pK_a is increased as a result. Thus, even though the site of mutation is in the middle of the Hb central cavity, its effects are communicated over a long distance to the DPG binding site.

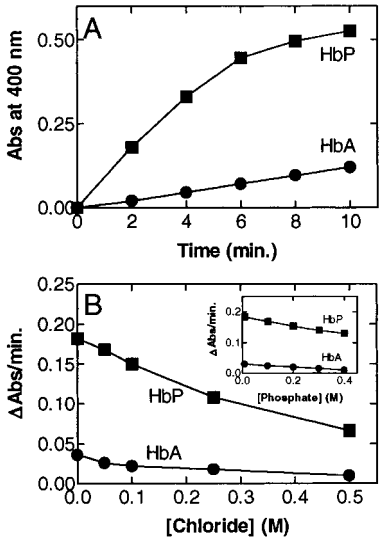

FIGURE 9: (A) Kinetics of the hydrolysis of *p*-NPA by oxyHbA and oxyHbP. The evolution of *p*-nitrophenol was followed at pH 7.4 in phosphate-buffered saline at room temperature by monitoring its absorption at 400 nm. Data were corrected for the background hydrolysis by the buffer. The concentration of *p*-NPA was 1 mM, and the concentration of Hb was 3 μM. (B) The influence of chloride ion concentration on the esterase activity of HbA and HbP. The rate of hydrolysis is expressed as the change in absorption at 400 nm per minute for the linear region of the kinetic data. The inset depicts the influence of phosphate buffer concentration.

Hydrolysis of p-Nitrophenyl Acetate. A comparison of the time-dependent hydrolysis of *p*-nitrophenyl acetate to *p*-nitrophenol and acetic acid by oxyHbA and oxyHbP (under identical conditions) is shown in Figure 9A. The rate of hydrolysis of the ester by HbP is approximately 5−6 times faster than that by HbA. The higher esterase activity of HbP was observed over a wide range of protein concentrations, and reflects the presence of significant differences between the conformational aspects of the $\beta\beta$ cleft in HbP and HbA.

The presence of chloride ions reduces the oxygen affinity of both HbA and HbP. The influence of increasing concentrations of chloride on the esterase activity of oxyHbA and oxyHbP is shown in Figure 9B. As the concentration of chloride is increased, the esterase activity of both proteins is reduced in a comparable manner. A similar decrease in the esterase activity is seen with an increase in the concentration of phosphate buffer (Figure 9B inset).

Gel filtration of the hydrolysis mixture after 30 min was used to quantify the *p*-nitrophenol liberated by HbA and HbP. Consistent with the results of the kinetic studies, HbP released nearly 5−6 times more *p*-nitrophenol than did HbA. The proteins, separated from the reactants and products by gel filtration, were then subjected to isoelectric focusing. The IEF pattern of HbP revealed that the 6-fold higher rate of hydrolysis of the ester (Figure 9A) was not accompanied by a higher level of irreversible acetylation of the protein (data not shown). Thus, the increased esterase activity of HbP appears to be achieved through an increase in the rate of a catalytic pathway (reversible acetylation) involving the participation of one or more His residues within the $\beta\beta$ cleft.

DISCUSSION

The experimental results presented here establish the differential sensitivity of the $\beta\beta$ cleft to effector analogue

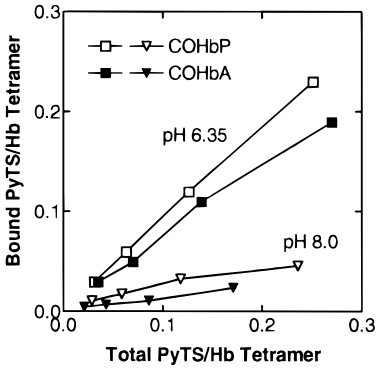

FIGURE 10: Titration of COHbA (black symbols) and COHbP (white symbols) (0.15−0.20 mM tetramer) with PyTS (5−40 μM) at pH 8.0 (50 mM Hepes) and pH 6.35 (50 mM bis-tris). The fraction of bound (quenched fluorescence lifetime) probe per hemoglobin tetramer is plotted vs the fraction of total added probe per tetramer. At pH 8.0, the CO-liganded proteins are expected to assume a normal R state conformation.

binding in HbPresbyterian and HbA. There are three principal differences between the binding of PyTS to HbP and HbA. The first observation is that the mutation in HbP (β108Asn → Lys), which is located in the interior of the protein approximately 15 Å from the $\beta\beta$ cleft, affects the binding of the effector analogue at the DPG binding pocket. The fact that there is any linkage between the mutation in the middle of the central cavity, with its additional positive charge, and the binding of effector molecules at the opening of the cavity implies long-range communication between these two well-separated sites. Second, the affinity of HbP for the PyTS ligand is consistently higher than the corresponding affinity of HbA under each of the solution conditions examined in this study. Even under conditions expected to produce R state hemoglobin (carbon monoxide ligation), as defined by the X-ray crystal structure (*10*), a difference in affinity for the probe is observed. At pH 8.0, COHbP possesses a greater affinity for the PyTS probe than does CO-ligated HbA (Figure 10). Both mutant and wild-type proteins exhibit a significantly lower affinity for probe by the DPG site in the R state (CO-liganded, pH 8.0) than in the deoxy-T or low-pH, CO-liganded (altered R) states. This result is also consistent with both proteins exhibiting the expected allosteric effect due to stabilization of the T state relative to the R state by the bound effector at the DPG site. Last, the mutation of β108 at the $\alpha_1\beta_1$ interface alters the normal dependence on pH for binding of effector analogues to the $\beta\beta$ cleft in deoxyHbP. These results have implications, consistent with the recently determined crystal structures of cross-bridged HbP (*9*), for understanding the mechanism whereby the ligation state of the hemes is transmitted into a change in the global quaternary state of the protein resulting in cooperative and allosteric ligand binding behavior.

One unexpected result based on the titration analysis presented here is that the PyTS probe binds to two independent sites with very different dissociation constants. It is most probable that the high-affinity site is, in fact, the DPG binding site found at the β-chain end of the central cavity. Previous effector binding results using the DPG analogue HPTS, which is closely related to PyTS, and steady state (*16*, *17*, *23*) or time-resolved (*4*) fluorescence indicate only a single binding site. Furthermore, competitive binding experiments with IHP show complete replacement of the HPTS with 1 mol of the IHP (*4*). However, in similar experiments with PyTS as the effector analogue, addition of IHP to both PyTS-bound HbA and HbP results in only partial replacement of the PyTS (D. S. Gottfried, A. S. Acharya, and J. M. Friedman, unpublished data). Conversely, if a sample of HbA or HbP is preloaded with a stoichiometric amount of IHP, titration with PyTS indicates that its preferred binding site is blocked and inaccessible, although some fraction of short-lived fluorescence is measured. This suggests that one binding site for PyTS is in the DPG pocket, where it can be displaced by added IHP, while the second as yet unknown site exists elsewhere within the Hb tetramer, and is immune to IHP binding. Other possible binding sites include the α end of the central cavity which is known to bind chloride ions, protons, and carbon dioxide, or the interior of the central cavity which has been shown to be the preferred binding site for effectors related to clofibric acid (*28*). We are examining these possibilities through additional competitive binding experiments. This apparent difference between the actions of PyTS and HPTS may possibly be due to the additional negative charge of PyTS (−4) compared to HPTS (−3) which would enhance the electrostatic interactions associated with binding.

The dissociation constants obtained using the fluorescence methods described here are qualitatively supported by other experimental studies of HbP. We have measured both UV and visible resonance Raman spectra of HbA and HbP in the absence and presence of added IHP, which binds strongly at the DPG pocket (*29*). UV Raman spectra of Hb, which are sensitive to the environment and H-bonding of the Tyr and Trp residues of the protein, exhibit characteristic features in the T and R states. Spectra of COHbP in the presence of 50 mM phosphate have many traits that are suggestive of a T-like quaternary state, even though the tetramer is fully ligated. The enhanced binding of effector analogues to HbP is further supported by visible Raman spectra of the heme groups. A lower stretching frequency of the proximal Fe−His bond is observed for HbP than for HbA when phosphate is bound in the DPG pocket. The decrease in the frequency of this Raman band is associated with a shift in quaternary structure toward a T-like state (*2*). NMR and resonance Raman measurements have also been taken for both HbP and the double recombinant mutant Hb(α96Val → Trp/β108Asn → Lys). Quaternary structure markers indicate that when the CO-ligated, R state forms of these Hbs are exposed to IHP they are switched to a T-like state (*30*). It has been suggested by Bonaventura et al. (*31*) that the additional positive charges in the central cavity introduced by the analogous β139Asn → Lys mutation (Hb Hinsdale) lead to repulsive interactions which widen the central cavity and result in lower oxygen affinity. A similar effect may be operative in HbP. Thus, the β108 region may be involved in the mechanism of ligand-induced communication across the $\alpha_1\beta_1$ interface.

The increased esterase activity of oxyHbP compared to oxyHbA further suggests that steric and/or electrostatic effects at the $\beta\beta$ cleft are influenced by the β108Asn → Lys mutation. Hb, like many other proteins, hydrolyzes *p*-nitrophenyl acetate. This catalytic activity is generally considered to be a reflection of the unique conformation of one or more surface His or Lys residues. In the case of Hb, this esterase activity has been suggested to be primarily

associated with the high density of positive charge in the $\beta\beta$ cleft region of Hb. Two of the four positively charged residues of the DPG binding pocket, namely, β2His and β82Lys, have been implicated as the functional groups responsible for the hydrolysis of *p*-nitrophenyl acetate. It has been suggested that catalytic hydrolysis of *p*-NPA by Hb is a useful probe of the conformational state of the $\beta\beta$ cleft (*15*).

Two modes of hydrolysis of the *p*-NPA have been postulated to explain the esterase activity of HbA (*15*). In one scheme, the β2His imidazole catalyzes the formation of a reversible intermediate (acyl Hb) that is subsequently hydrolyzed to acetate and Hb. No irreversible modification of the protein takes place in this catalytic mode of hydrolysis. The second scheme involves the irreversible modification of the protein requiring the participation of β82Lys and formation of a stable acetylated Lys residue. Since the formation of an acetylated Lys residue results in the loss of some positive charge of the protein, an isoelectric focusing gel of the protein incubated with *p*-NPA can provide a quantification of the protein involved in this reaction. The IEF indicates that only the reversible, catalytic process is accelerated in HbP, and this leads to the conclusion that β2His is perturbed either conformationally or electrostatically by the presence of the β108Lys mutation. Although the altered pH dependence of PyTS binding to the deoxy proteins (Figure 8) is suggestive of an altered pK_a for a His residue (β2 or β143) in HbP, the exact mechanism by which the additional positive charge in the central cavity accomplishes this change over such a long distance is uncertain.[4] In particular, since the X-ray crystallographic deoxy conformations of both HbA and HbP appear to be the canonical T state (*9*), subtle differences in hydrogen bonding, salt bridges, and/or equilibrium conformational states dynamics must be responsible for the observed action at a distance.

The effector analogue binding results presented here suggest that, whereas in HbA there is a connection between the occupancy of the heme ligand binding sites and the conformation at the β end of the central cavity, in the mutant HbP there appears to be some decoupling of the heme ligation state and the affinity of the DPG binding site for effector molecules. The high-pH, CO-liganded R states of both mutant and wild-type proteins exhibit little affinity for the effector analogue (Figure 10), consistent with the X-ray crystallographic structure of R state-liganded hemoglobin which reveals a central cavity that cannot readily accommodate the binding of effectors in the DPG binding site. However, the difference in the extent of analogue binding between the deoxy T state and the low pH, CO-liganded state observed for HbA is not seen in HbP (Figure 7 and Table 1). The X-ray crystallographic B structure, observed for the liganded (cyanomet) derivative of the glycine cross-bridged variant of HbP (*9*), provides a plausible framework for understanding the origin of this decoupling. The B structure has several features distinct from the previously described R and T structures (*10*, *13*). The B state heme sites are at least partially relaxed from the deoxy T state tertiary conformation toward the normal liganded R state conformation. Upon switching from the T to the R quaternary structure, the central cavity undergoes a change in dimensions which leaves the β end narrower while the α end is slightly expanded. The substantial decrease in the affinity of effectors for binding to the DPG site in R state Hb is attributed to this reduction in the size of the β end of the central cavity. This preferential binding can also be viewed as the source of stabilization of the T state by the presence of DPG or analogue effectors.

The change in the DPG pocket which accompanies the T $\rightarrow$ R transition arises from a screw axis located between the dimers at a point near the α end of the central cavity which allows the $\alpha\beta$ dimers to rotate (13.5°) and translate (1.5 Å) with respect to one another. In contrast, the screw axis associated with the T $\rightarrow$ B transition is located closer to the β end of the central cavity and is rotated by nearly 90° from the T $\rightarrow$ R screw axis. Thus, ligand binding at the hemes results in only an 8.7° rotation and 0.1 Å translation of the dimers, producing significantly reduced changes at the DPG binding site (J. Kavanaugh and A. Arnone, personal communication). The B structure also retains many T state-like interactions within the $\alpha_1\beta_2$ interface. Thus, the B structure is likely to have a moderately high oxygen affinity (intermediate between T and R) even though it displays several T state-like features, including the accessible and accommodating DPG binding site.

The binding of organic phosphates to liganded Hb has been observed in earlier studies (*32*, *33*) and was used to conclude that there is a dynamic equilibrium between different ligand-bound quaternary structures: those which allow effector binding (open central cavity) and those which are resistant to effector binding (closed central cavity). Many of the spectroscopic and functional properties of solution-phase liganded hemoglobins in the presence of DPG-type effectors can be explained by assuming that it is, in fact, the B and R state structures which are in equilibrium. In the absence of effectors or at high pH, the predominant species is R (or R2); however, upon binding of an effector to the DPG site, the B structure predominates. The difference between liganded HbA and liganded HbP is likely to be the relative stability of the B state compared to that of the R state. The PyTS binding results presented in this study are a natural consequence if, in HbP compared to HbA, the B state is more stable and is more readily accessible (lower energy barrier for formation) from the R state. Thus, the Hb tetramer's binding affinity for allosteric effectors (and analogues) is not determined primarily by the ligation state of the hemes (oxy vs deoxy) but rather by the quaternary state of the tetramer and how this dictates the conformation of the effector binding site and its electrostatic interactions with substrate.

A model, based on X-ray structural data for several Hb variants with mutations at the β37Trp residue (*34*), is proposed which is consistent with our observations. These oxygen-ligated β37 mutants appear to exist in a B state quaternary conformation analogous to the cyanomet derivative of HbP observed by Kroeger and Kundrot (*9*). The study of these high-affinity T-like states in Hb is being used to separate the quaternary state-induced structural changes from those induced by ligand binding within the T state. Arnone suggests that through a sequence of tertiary conformational changes starting at the heme iron atom and leveraged into a

[4] Preliminary experiments in our lab, using UV resonance Raman spectroscopy to measure the number of protonated histidine residues (*36*), provide evidence of a qualitative difference between HbA and HbP as a function of pH.

1.5 Å movement of the FG corner, ligation of the α-globin heme produces a bending of the $\alpha\beta$ dimers which destabilizes the hinge region of the $\alpha_1\beta_2$ interface and facilitates the quaternary state reorganization. The degree of dimer bending is directly correlated with the magnitude of dimer rotation about the screw axis which alters the DPG pocket. The residue at β108 is intimately involved in the bending of the $\alpha\beta$ dimer, so mutation at that region likely leads to a perturbation in the ligation-induced hinge motions. The lysine mutation at β108 in HbP forms a new hydrogen bond with Tyrβ35 in the deoxy state which is broken in the transition to the liganded form of the protein (*9*). In the B state, Lysβ108 is exposed to the solvent of the central cavity. Conceivably, this alteration in the $\alpha_1\beta_1$ hinge region could lead to a lower barrier for the formation of the B structure from the liganded R state and to greater stability for this conformation once it is formed. An alternative mechanism for releasing ligand binding-induced strain is also supported by observations with crystals of HbP. Crystals of deoxyHbA, on exposure to air, are shattered by the disordering induced by the T → R quaternary transition. Neither deoxyHbA in the presence of the effector IHP nor deoxyHbP (without bound effector) shatters with air exposure, indicating that HbP, like effector-bound HbA, is predisposed to maintaining a T-like ligand-bound quaternary state, namely, the B state. Likewise, crystals of the deoxy T state β37 mutants, upon exposure to oxygen, exhibit only small quaternary state changes and remain T-like. It may be that mutations at both β108 and β37 in human Hb result in high-affinity, T-like liganded structures (B state) through similar, though distinct, mechanisms: in the former through loss of communication across the $\alpha_1\beta_1$ hinge region and in the latter through a weakened or disrupted $\alpha_1\beta_2$ interface.

In summary, the mutation within the $\alpha_1\beta_1$ dimer interface of HbPresbyterian appears to have long-range structural and/or electrostatic consequences that can be monitored through the accessibility of a DPG analogue to the binding pocket at the $\beta\beta$ cleft of the central cavity. The quaternary state conformational change due to ligand binding at the heme groups in hemoglobin is the result of a sequence of finely tuned changes in amino acid positions. Disruption of this mechanism through mutation allows the protein to populate conformational states, such as a high-affinity T state, that are not normally accessible but which exist within the dynamic families of the R and T structures.

ACKNOWLEDGMENT

We thank Drs. Eric Peterson, Laura Juszczak, Celia Bonaventura, Jeff Kavanaugh, Arthur Arnone, and Chien Ho for fruitful discussions and access to unpublished data. We also acknowledge the reviewers for helpful comments and suggestions.

REFERENCES

1. Benesch, R., and Benesch, R. E. (1967) *Biochem. Biophys. Res. Commun. 26*, 162−167.
2. Friedman, J. M., Scott, T. W., Stepnoski, R. A., Ikeda-Saito, M., and Yonetani, T. (1983) *J. Biol. Chem. 258*, 10564−10572.
3. Scott, T. W., and Friedman, J. M. (1984) *J. Am. Chem. Soc. 106*, 5677−5687.
4. Gottfried, D. S., Juszczak, L. J., Fataliev, N. A., Acharya, A. S., Hirsch, R. E., and Friedman, J. M. (1997) *J. Biol. Chem. 272*, 1571−1578.
5. Peterson, E. S., and Friedman, J. M. (1998) *Biochemistry 37*, 4346−4357.
6. Moo-Penn, W. F., Wolff, J. A., Simon, G., Vacek, M., Jue, D. L., and Johnson, M. H. (1978) *FEBS Lett. 92*, 53−56.
7. O'Donnell, J. K., Birch, P., Parsons, C. T., White, S. P., Okabe, J., Martin, M. J., Adams, C., Sundarapandiyan, K., Manjula, B. N., Acharya, A. S., Logan, J. S., and Kumar, R. (1994) *J. Biol. Chem. 269*, 27692−27699.
8. Looker, D., Abbott-Brown, D., Cozart, P., Durfee, S., Hoffman, S., Mathews, A. J., Miller-Roehrich, J., Shoemaker, S., Trimble, S., Fermi, G., Komiyama, N. H., Nagai, K., and Stetler, G. L. (1992) *Nature 356*, 258−260.
9. Kroeger, K. S., and Kundrot, C. E. (1997) *Structure 5*, 227−237.
10. Shaanan, B. (1983) *J. Mol. Biol. 171*, 31−59.
11. Silva, M. M., Rogers, P. H., and Arnone, A. (1992) *J. Biol. Chem. 267*, 17248−17256.
12. Smith, F. R., Lattman, E. E., and Carter, C. W. J. (1991) *Proteins: Struct., Funct., Genet. 10*, 81−91.
13. Fermi, G., Perutz, M. F., Shaanan, B., and Fourme, R. (1984) *J. Mol. Biol. 175*, 159−174.
14. Elbaum, D., and Nagel, R. L. (1981) *J. Biol. Chem. 256*, 2280−2283.
15. Elbaum, D., Wiedenmann, B., and Nagel, R. L. (1982) *J. Biol. Chem. 257*, 8454−8458.
16. Gibson, Q. H., and MacQuarrie, R. (1971) *J. Biol. Chem. 246*, 5832−5856.
17. MacQuarrie, R., and Gibson, Q. H. (1972) *J. Biol. Chem. 247*, 5686−5694.
18. Antonini, E., and Brunori, M. (1971) *Hemoglobin and Myoglobin in their Reactions with Ligands*, North-Holland Publishing Co., Amsterdam.
19. Gottfried, D. S., Peterson, E. S., Sheikh, A. G., Wang, J., Yang, M., and Friedman, J. M. (1996) *J. Phys. Chem. 100*, 12034−12042.
20. Eisinger, J., and Flores, J. (1979) *Anal. Biochem. 94*, 15−21.
21. Grinvald, A., and Steinberg, I. Z. (1974) *Anal. Biochem. 59*, 583−598.
22. Johnson, M. L., and Frasier, S. G. (1985) *Methods Enzymol. 117*, 301−342.
23. Serbanescu, R., Kiger, L., Poyart, C., and Marden, M. C. (1998) *Biochim. Biophys. Acta 1363*, 79−84.
24. van Holde, K. E. (1985) *Physical Biochemistry*, 2nd ed., Prentice-Hall, Englewood Cliffs, NJ.
25. Gryczynski, Z., Fronticelli, C., Tenenholz, T., and Bucci, E. (1993) *Biophys. J. 65*, 1951−1958.
26. Gryczynski, Z., Lubkowski, J., and Bucci, E. (1997) *Methods Enzymol. 278*, 538−569.
27. Pines, E., and Huppert, D. (1986) *Chem. Phys. Lett. 126*, 88−91.
28. Lalezari, I., Lalezari, P., Poyart, C., Marden, M., Kister, J., Bohn, B., Fermi, G., and Perutz, M. F. (1990) *Biochemistry 29*, 1515−1523.
29. Peterson, E. S., Wang, J., Gottfried, D. S., Huang, S., Acharya, S., and Friedman, J. M. (1996) *Biophys. J. 70*, A112.
30. Ho, C., Sun, D. P., Shen, T.-J., Ho, N. T., Zou, M., Hu, C.-K., Sun, Z.-Y., and Lukin, J. A. (1997) in *Present and Future Perspectives of Blood Substitutes* (Tsuchida, E., Ed.) Elsevier Science SA, Lausanne, Switzerland.
31. Bonaventura, C., Arumugam, A., Cashon, R., Bonaventura, J., and Moo-Penn, W. F. (1994) *Biophys. J. 66*, A270.
32. Adams, M. L., and Schuster, T. M. (1974) *Biochem. Biophys. Res. Commun. 58*, 525−531.
33. Coletta, M., Ascenzi, P., Castagnola, M., and Giardina, B. (1995) *J. Mol. Biol. 249*, 800−803.
34. Kavanaugh, J. S., Weydert, J. A., Rogers, P. H., and Arnone, A. (1998) *Biochemistry 37*, 4358−4373.
35. Gutman, M., Nachliel, E., and Huppert, D. (1982) *Eur. J. Biochem. 125*, 175−181.
36. Zhao, X., Wang, D., and Spiro, T. G. (1998) *J. Am. Chem. Soc. 120*, 8517−8518.

BI9827464